Identification of novel and distinct FGF23 signaling in a Klotho-dependent and -independent manner

Klaudia Kopper[1,2], Johanne Pastor[4], Orson W. Moe[3,4,5], Johannes Loffing[1,2], Ganesh Pathare[1,2]*

[1]Institute of Anatomy, University of Zurich, Zurich, Switzerland
[2]Swiss National Centre of Competence in Research "Kidney Control of Homeostasis", Switzerland
[3]Charles and Jane Pak Center for Mineral Metabolism and Clinical Research, University of Texas Southwestern Medical Center, Dallas, Texas, USA.
[4]Departments of Internal Medicine, University of Texas Southwestern Medical Center, Dallas, Texas, USA.
[5]Departments of Physiology, University of Texas Southwestern Medical Center, Dallas, Texas, USA.

***Corresponding author**:
Ganesh Pathare
Institute of Anatomy
University of Zurich
Winterthurerstrasse 190, 8057, CH
Email: ganesh.pathare@anatomy.uzh.ch

Keywords: FGF23, Klotho, chronic kidney disease, left ventricular hypertrophy and inflammation

Competing Interests

The authors declare no potential conflicts of interest.

ABSTRACT

Fibroblast growth factor-23 (FGF23) is crucial for phosphate and vitamin D homeostasis. Moreover, FGF23 levels are very high in patients with chronic kidney disease (CKD) with unclear functions. Binding of FGF23 to its coreceptor Klotho is considered essential for its actions. However, recent data suggested that CKD-related high FGF23 levels may have Klotho-independent cardiotoxic and inflammatory effects but the underlying signaling mechanisms are unclear. Here, we performed a comprehensive and unbiased transcriptomic profiling in HEK293 cells, comparing the effects of 0.5 nM FGF23 for 1 hour (low-transitory: ~physiological) and 10 nM FGF23 for 24 hours (high-prolonged: ~pathological), in the presence and absence of Klotho. We found that, at physiological concentration, FGF23 action requires Klotho and follows the canonical MAPK signaling. Conversely, at pathological high levels, FGF23 acts both in the presence and in the absence of Klotho. In the presence of Klotho, high FGF23 activates a plethora of transcripts including the inflammatory genes (e.g. *TGFB1, GDF15, ANXA1* and *TNFRSF9/12*) known to be elevated in patients with CKD. Interestingly, in the absence of Klotho, high FGF23 levels does also regulate a small and unique set of genes related to post-transcriptional modifications and translation initiation. To conclude, Klotho is essential for FGF23 signaling at physiological FGF23 concentrations. However, with pathologically high FGF23 levels, Klotho acts as a molecular switch determining the type of FGF23 response.

INTRODUCTION:

Mammalian endocrine fibroblast growth factors (FGFs), unlike paracrine ones, have a low affinity for heparan sulfate and need additional co-receptors for function. Bone-derived FGF23 requires αKlotho (Klotho) along with the FGF receptor (FGFR) to act in target tissues[1,2]. Three FGFRs (FGFR1c, FGFR3c, FGFR4) are known to mediate FGF23 actions. The FGF23/FGFR/Klotho complex regulates phosphate and vitamin D homeostasis in all mammals. However, recent studies indicate that in chronic kidney disease (CKD), excess FGF23 directly activates FGFR4 in the heart[3,4] and liver[5] without needing Klotho, leading to left ventricular hypertrophy (LVH) and inflammation, respectively. These direct actions of FGF23 contradict the recent functional and structural data that support the essential role of transmembrane or circulatory soluble-Klotho in FGF23 actions through FGFR1 and FGFR4[1,2].

Physiological regulators like dietary phosphate, $1,25(OH)_2D_3$ and PTH stimulate FGF23 transiently within a narrow limit[6]. In contrast, CKD is linked to consistently high FGF23 levels[6].
The differential effects of low-transitory (~physiological) versus high-prolonged (~pathological) FGF23 levels, in the context of Klotho, are unclear. Despite FGF23 being known to directly regulate many genes (e.g. *EGR1* and *FOS*), its effect on transcriptomic responses using RNA-seq is underexplored. We hypothesized that physiological and pathological FGF23 concentrations, with or without Klotho, may drive distinct transcriptomic responses, potentially revealing FGF23 signaling in health and CKD. To this end, we employed HEK293 cells, an excellent model[1,4] that lacks endogenous Klotho but expresses three necessary FGFRs to study FGF23 signaling.

RESULTS AND DISCUSSION

1. Sustained activation of canonical signaling by high, but not low, FGF23 concentrations.

As previously reported[1], a minimum FGF23 concentration of 0.5 nM (~16 ng/ml) is required to activate canonical signaling in Klotho-expressing HEK293 cells ($HEK293^{Kl}$). We found that *EGR1* mRNA peaked at 1 hour with no difference at 24 hours in 0.5 nM FGF23 treated *versus* untreated $HEK293^{Kl}$ cells (Fig. 1A). Interestingly, 10 nM FGF23 (~320 ng/ml) treatment followed almost a similar trend except a 13-fold higher *EGR1* was still observed after 24 hours (Fig. 1A/B). *EGR1* mRNA levels remained unchanged in $HEK293^{Wt}$ cells throughout the treatment periods. Similarly, as shown in fig. 1C, treatment with 0.5 nM FGF23 in $HEK293^{Kl}$ cells resulted in an increase in pERK1/2 visible after 15 minutes, but not at 24 hours. Conversely, 10 nM FGF23 treatment led to pERK1/2 activation at both 15 minutes and 24 hours. The sustained activation of *EGR1*/ERK, resulting from prolonged exposure to high levels of FGF23, may be relevant in CKD patients, whose FGF23 levels are 5-100 times higher depending on the stage of the disease. To discern the impact of transient *versus* sustained ERK activation and any Klotho-independent effects of FGF23, we performed transcriptomics profiling as shown in fig. 1D.

110 **2. Lack of transcriptomics response to low-transitory FGF23 without Klotho.**
111 As depicted in fig. 1E, low-transitory FGF23 significantly altered the expression of more than 350
112 genes in the presence of Klotho, while in the absence of Klotho, FGF23 failed to alter the
113 expression of a single gene (dataset S1/2). We further analyzed the transcriptomic response to
114 Klotho by applying a threshold of log2FC>1. With this threshold, 61 genes were upregulated and
115 3 genes were downregulated as highlighted in the volcano plot shown in fig. 1F. Notably, canonical
116 FGF23 targets such as *EGR1, FOS*, and *DUSP* were among the top upregulated genes, validating
117 our approach (Fig. 1H). Moreover, subsequent Gene ontology (GO) analysis confirmed the
118 predominant activation of the canonical MAPK pathway (Fig. 1I, dataset S3).
119
120 Our results align with recent crystal structure and functional studies demonstrating that Klotho is
121 essential for in the physiological actions of FGF23[1,2]. However, earlier studies in HEK293 and
122 hepatocytes found that FGF23 may up-regulate PLCγ within 30 minutes of treatment without
123 Klotho[4,5]. It's may possible that this effect isn't mirrored at the mRNA level at a particular time-point
124 and therefore we couldn't observe any response.
125
126 **3. High-prolonged FGF23 upregulates several CKD markers with Klotho but regulates a**
127 **separate set of genes without Klotho.**
128 The volcano plots in fig. 2A and B depict a strong response to high-prolonged FGF23 in the
129 presence of Klotho but only a modest response in the absence of Klotho (dataset S4/5). The Venn
130 diagram in fig. 2C shows that when comparing Klotho-positive and -negative cells, only 5
131 transcripts were shared among all upregulated transcripts, and 7 were shared among all
132 downregulated transcripts. This indicates minimal overlap in the signaling pathways activated by
133 high-prolonged FGF23 in the presence *versus* in absence of Klotho. Furthermore, the top 5 up-
134 and downregulated genes in Klotho-negative cells remained either unchanged or showed
135 significant opposite regulation when Klotho was present, suggesting that Klotho may act as a
136 molecular switch decisive for the type of FGF23 signaling (Fig. 2D, dataset S6). GO analysis
137 suggested that high-prolonged FGF23 without Klotho regulates mainly post-transcriptional
138 modification and translation initiation pathways. The full list of pathways implicated is included in
139 dataset S7.
140
141 As depicted in the Venn diagram in fig. 2E, we identified 88 differently-regulated genes that are
142 upregulated in the presence of Klotho only with high-prolonged but not with low-transitory FGF23.
143 Many gene products of these unique 'pathological' FGF23 targets were previously linked to
144 inflammation and immune responses in patients with CKD (Fig. 2F). Transforming growth factor
145 beta 1 (*TGFB1)* is thought to mediate renal fibrosis in diabetic nephropathy and CKD via activation
146 of intracellular SMAD proteins[7]. Tumor necrosis factor receptor superfamily member 9 and 12A
147 (*TNFRSF9*/*TNFRSF12A)* are proinflammatory receptors known to contribute to kidney
148 inflammation through canonical and non-canonical NFκB activation[8]. Likewise, Annexin A1
149 (*ANXA1*) gets up-regulated in patients with diabetic nephropathy, and its levels appear to be

negatively correlated with kidney function and kidney outcomes[9]. Growth differentiation factor-15 (*GDF15)* is part of the TGF-β cytokine superfamily and renal GDF15 expression and plasma levels associates with the decline of kidney function in CKD patients[10]. *ATF4* and *PSAT1* are not directly implicated in human CKD but play crucial roles in vascular calcification[11] and serine biosynthesis associated-inflammation[12], respectively. Dataset S8 includes a full list of these FGF23-targets.

Presently it is unclear whether elevated FGF23 and inflammatory response in CKD are beneficial or detrimental to the disease progression. Although it is anticipated that high FGF23 levels in CKD patients may upregulate these transcripts via sustained ERK activation, the *in-vitro* nature of our study could not verify this. The surprising, yet plausible observation that Klotho is needed for the inflammatory/immune response by high-prolonged FGF23 underscores the complexity of the FGF23-Klotho axis. CKD is considered a state of circulatory-Klotho deficiency, however, the remaining circulatory or tissue Klotho still may trigger these effects. Previous reports have confirmed that elevated FGF23 requires Klotho to exert its 'untoward' effects[13,14]. High FGF23 in CKD patients may contribute to bone loss by directly sustained ERK activation in bone cells only in the presence of Klotho[13,14]. Very high circulatory Klotho levels in conjunction with FGF23 cause osteomalacia probably due to sustained ERK activation[15,16].

The strength of our study lies in identifying distinct signaling by low and high FGF23 levels in Klotho dependent and independent manner. Nonetheless, our study also has some limitations. First, it is surmised that, in the presence of Klotho, transient and sustained ERK activation by low-transitory and high-prolonged FGF23, respectively, may have caused observed transcriptomic responses. However, the precise mechanisms are still unclear. Moreover, the process by which high-prolonged FGF23 without Klotho induces transcriptomic responses remains to be elucidated. Second, as with any *in-vitro* data, our results need to be verified through elaborate *in-vivo* studies.

In conclusion, our study suggests mainly Klotho-dependent FGF23 actions in physiological conditions. The pathologically high and prolonged FGF23 levels seem to induce inflammatory and immune responses primarily in the presence of Klotho. The absence of Klotho results in modest and distinct transcriptomics response to pathological FGF23 levels. Overall, Klotho serves as a key molecular switch, delineating the differential responses to physiological and pathological FGF23 levels.

MATERIAL AND METHODS

Detailed descriptions are provided in *SI Appendix.*

FUNDING AND ADDITIONAL INFORMATION

This work is supported by the Swiss National Science Foundation through the National Center of Competence in Research NCCR Kidney.CH. [grant number N-403-03-55 (to Ganesh Pathare)].

AUTHORS CONTRIBUTIONS

GP conceptualized and designed the study; KK and GP performed the study; JP, OM and JL contributed new reagents and tools; KK and GP analyzed data and wrote the paper; JP, OM and JL reviewed and edited the manuscript; GP was responsible for supervision and funding acquisition.

228 **REFERNCES**

229 1. Chen, G., Liu, Y., Goetz, R., Fu, L., Jayaraman, S., Hu, M. C., Moe, O. W., Liang, G., Li,
230 X. & Mohammadi, M. α-Klotho is a non-enzymatic molecular scaffold for FGF23 hormone
231 signalling. *Nature* **553**, 461–466 (2018).

232 2. Chen, L., Fu, L., Sun, J., Huang, Z., Fang, M., Zinkle, A., Liu, X., Lu, J., Pan, Z., Wang, Y.,
233 Liang, G., Li, X., Chen, G. & Mohammadi, M. Structural basis for FGF hormone signalling.
234 *Nature* **618**, 862–870 (2023).

235 3. Faul, C., Amaral, A. P., Oskouei, B., Hu, M. C., Sloan, A., Isakova, T., Gutiérrez, O. M.,
236 Aguillon-Prada, R., Lincoln, J., Hare, J. M., Mundel, P., Morales, A., Scialla, J., Fischer,
237 M., Soliman, E. Z., Chen, J., Go, A. S., Rosas, S. E., Nessel, L., *et al.* FGF23 induces left
238 ventricular hypertrophy. *J. Clin. Invest.* **121**, 4393–4408 (2011).

239 4. Grabner, A., Amaral, A. P., Schramm, K., Singh, S., Sloan, A., Yanucil, C., Li, J.,
240 Shehadeh, L. A., Hare, J. M., David, V., Martin, A., Fornoni, A., Di Marco, G. S., Kentrup,
241 D., Reuter, S., Mayer, A. B., Pavenstädt, H., Stypmann, J., Kuhn, C., *et al.* Activation of
242 Cardiac Fibroblast Growth Factor Receptor 4 Causes Left Ventricular Hypertrophy. *Cell*
243 *Metab.* **22**, 1020–1032 (2015).

244 5. Singh, S., Grabner, A., Yanucil, C., Schramm, K., Czaya, B., Krick, S., Czaja, M. J., Bartz,
245 R., Abraham, R., Di Marco, G. S., Brand, M., Wolf, M. & Faul, C. Fibroblast growth factor
246 23 directly targets hepatocytes to promote inflammation in chronic kidney disease. *Kidney*
247 *Int.* **90**, 985–996 (2016).

248 6. Edmonston, D., Grabner, A. & Wolf, M. FGF23 and klotho at the intersection of kidney and
249 cardiovascular disease. *Nat. Rev. Cardiol. 2023* 1–14 (2023) doi:10.1038/s41569-023-
250 00903-0.

251 7. Meng, X. M., Nikolic-Paterson, D. J. & Lan, H. Y. TGF-β: the master regulator of fibrosis.
252 *Nat. Rev. Nephrol. 2016 126* **12**, 325–338 (2016).

253 8. Sanz, A. B., Sanchez-Nĩo, M. D. & Ortiz, A. TWEAK, a multifunctional cytokine in kidney
254 injury. *Kidney Int.* **80**, 708–718 (2011).

255 9. Wu, L., Liu, C., Chang, D. Y., Zhan, R., Sun, J., Cui, S. H., Eddy, S., Nair, V., Tanner, E.,
256 Brosius, F. C., Looker, H. C., Nelson, R. G., Kretzler, M., Wang, J. C., Xu, M., Ju, W.,
257 Zhao, M. H., Chen, M. & Zheng, L. Annexin A1 alleviates kidney injury by promoting the
258 resolution of inflammation in diabetic nephropathy. *Kidney Int.* **100**, 107 (2021).

259 10. Nair, V., Robinson-Cohen, C., Smith, M. R., Bellovich, K. A., Bhat, Z. Y., Bobadilla, M.,
260 Brosius, F., De Boer, I. H., Essioux, L., Formentini, I., Gadegbeku, C. A., Gipson, D.,
261 Hawkins, J., Himmelfarb, J., Kestenbaum, B., Kretzler, M., Magnone, M. C., Perumal, K.,

262 Steigerwalt, S., *et al.* Growth Differentiation Factor-15 and Risk of CKD Progression. *J.*
263 *Am. Soc. Nephrol.* **28**, 2233–2240 (2017).

264 11. Masuda, M., Miyazaki-Anzai, S., Keenan, A. L., Okamura, K., Kendrick, J., Chonchol, M.,
265 Offermanns, S., Ntambi, J. M., Kuro-O, M. & Miyazaki, M. Saturated phosphatidic acids
266 mediate saturated fatty acid–induced vascular calcification and lipotoxicity. *J. Clin. Invest.*
267 **125**, 4544–4558 (2015).

268 12. Wang, J., Filippakis, H., Hougard, T., Du, H., Ye, C., Liu, H. J., Zhang, L., Hindi, K.,
269 Bagwe, S., Nijmeh, J., Asara, J. M., Shi, W., El-Chemaly, S., Henske, E. P. & Lam, H. C.
270 Interleukin-6 mediates PSAT1 expression and serine metabolism in TSC2-deficient cells.
271 *Proc. Natl. Acad. Sci. U. S. A.* **118**, e2101268118 (2021).

272 13. Shalhoub, V., Ward, S. C., Sun, B., Stevens, J., Renshaw, L., Hawkins, N. & Richards, W.
273 G. Fibroblast growth factor 23 (FGF23) and alpha-klotho stimulate osteoblastic MC3T3.E1
274 cell proliferation and inhibit mineralization. *Calcif. Tissue Int.* **89**, 140–150 (2011).

275 14. Komaba, H., Kaludjerovic, J., Hu, D. Z., Nagano, K., Amano, K., Ide, N., Sato, T.,
276 Densmore, M. J., Hanai, J. ichi, Olauson, H., Bellido, T., Larsson, T. E., Baron, R. &
277 Lanske, B. Klotho expression in osteocytes regulates bone metabolism and controls bone
278 formation. *Kidney Int.* **92**, 599–611 (2017).

279 15. Brownstein, C. A., Adler, F., Nelson-Williams, C., Iijima, J., Li, P., Imura, A., Nabeshima,
280 Y. I., Reyes-Mugica, M., Carpenter, T. O. & Lifton, R. P. A translocation causing increased
281 α-Klotho level results in hypophosphatemic rickets and hyperparathyroidism. *Proc. Natl.*
282 *Acad. Sci. U. S. A.* **105**, 3455–3460 (2008).

283 16. Smith, R. C., O'Bryan, L. M., Farrow, E. G., Summers, L. J., Clinkenbeard, E. L., Roberts,
284 J. L., Cass, T. A., Saha, J., Broderick, C., Ma, Y. L., Zeng, Q. Q., Kharitonenkov, A.,
285 Wilson, J. M., Guo, Q., Sun, H., Allen, M. R., Burr, D. B., Breyer, M. D. & White, K. E.
286 Circulating αKlotho influences phosphate handling by controlling FGF23 production. *J.*
287 *Clin. Invest.* **122**, 4710–4715 (2012).

288

289
290
291
292
293
294
295
296

FIGURE LEGENDS

Fig. 1. i) Effects of low versus high FGF23 concentrations on canonical signaling.

A) Fold change *EGR1* mRNA levels, normalized to *GAPDH* upon treating 0.5 nM and 10 nM FGF23 in HEK293^{Kl} and HEK293^{Wt} cells over 24 hours (n=3). *p* values in red and teal indicate comparisons between FGF23 vs control treatment in HEK293^{Kl} and HEK293^{Wt} cells, respectively. ns=p>0.05. **B)** *EGR1* mRNA, normalized to *GAPDH,* upon treating 0.5 nM and 10 nM FGF23 for 24 hours in HEK293^{Kl} cells (n=3). **C)** Original immunoblots of Klotho, pERK1/2 and tERK1/2 upon treating 0.5 nM and 10 nM FGF23 in HEK293^{Kl} and HEK293^{Wt} cells for 15 min and 24 hrs. **D)** Transcriptomics study plan.

ii) Transcriptomics response to low-transitory FGF23.

E) DEG counts upon low-transitory FGF23 in the presence (HEK293^{Kl}) and absence of Klotho (HEK293^{Wt}). **F&G)** Volcano plots of all the genes upon low-transitory FGF23 in the presence and absence of Klotho, respectively. The up and downregulated genes with log2FC>1 are shown in red and blue respectively. **H)** Top 15 upregulated genes upon low-transitory FGF23 in the presence of Klotho (n=3). **J)** Selected upregulated GO pathways upon low-transitory FGF23 with Klotho. All the values are expressed as arithmetic means ± SD.

Fig. 2. Transcriptomics response to high-prolonged FGF23.

A) Volcano plot of all the genes upon high-prolonged FGF23 in the presence of Klotho (HEK293^{Kl}). Significantly up and downregulated genes with log2FC>1 are shown in red and blue respectively. **B)** Volcano plot of all the genes upon high-prolonged FGF23 in the absence of Klotho (HEK293^{Wt}). All significantly expressed genes, depicted in green and exhibit a log2FC<1. **C)** Venn diagrams showing significantly up and downregulated genes (padj<0.05) in the presence or absence of Klotho. **D)** Top 5 up and downregulated genes upon high-prolonged FGF23 in the absence of Klotho (orange bars). Note that these transcripts are either unchanged or oppositely regulated when Klotho is present (grey bars). **E)** Venn diagram showing DEG (padj<0.05) compared between low-transitory FGF23 and high-prolonged FGF23 in the presence of Klotho. **F)** Unique genes upregulated only by high-prolonged FGF23 in the presence of Klotho (red bars). Note that these genes are unchanged when Klotho was absent (grey bars). (n=3). *=padj<0.05, ns=padj>0.05. All the values are expressed as arithmetic means ± SD. **G)** Proposed model illustrating Klotho as a molecular switch regulating FGF23 actions in health and disease.

Fig. 1

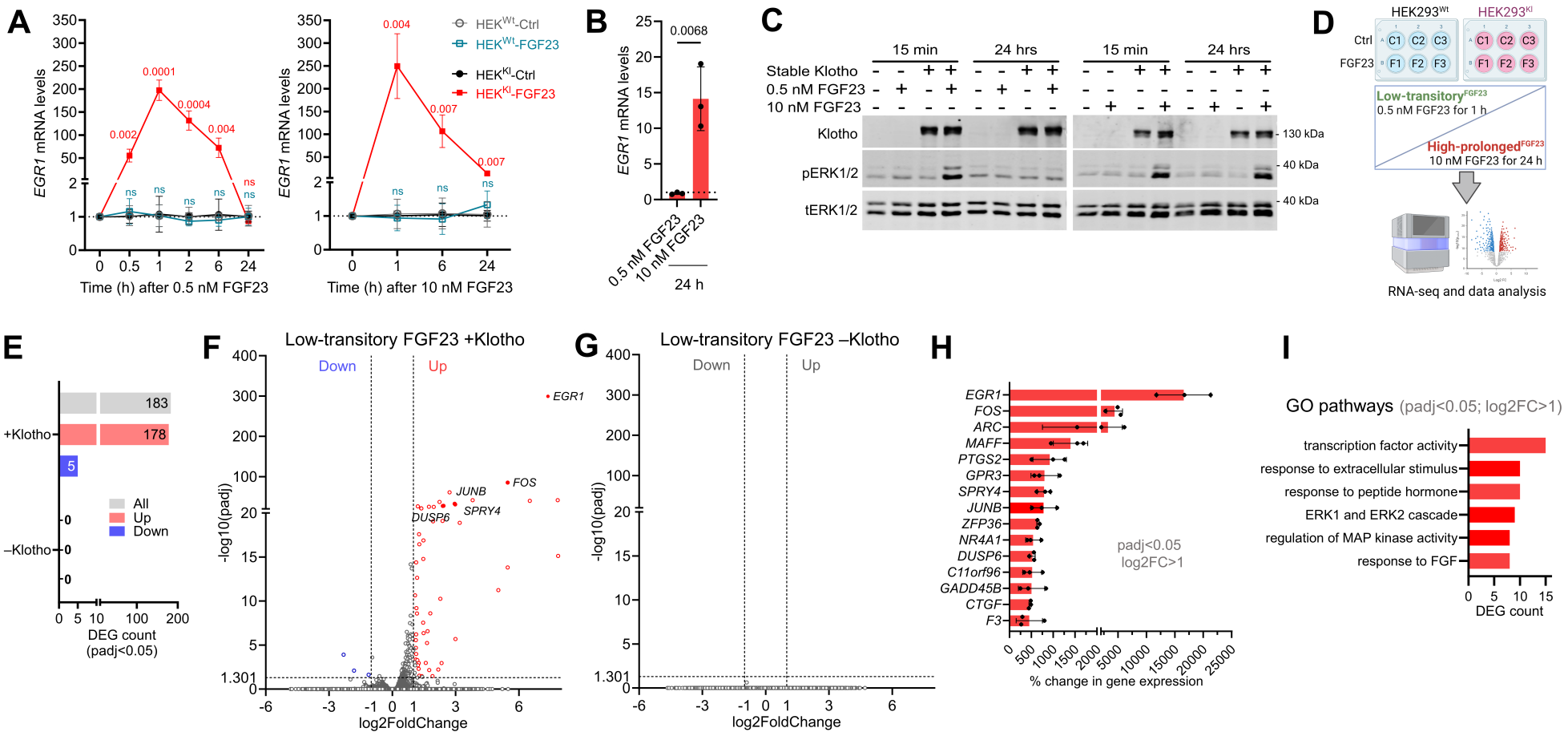
A
EGR1 mRNA levels
Time (h) after 0.5 nM FGF23
Time (h) after 10 nM FGF23
HEKWt-Ctrl
HEKWt-FGF23
HEKKl-Ctrl
HEKKl-FGF23
B
0.0068
0.5 nM FGF23
10 nM FGF23
24 h
C
15 min
24 hrs
Stable Klotho
0.5 nM FGF23
10 nM FGF23
Klotho
pERK1/2
tERK1/2
130 kDa
40 kDa
D
HEK293Wt
HEK293Kl
Ctrl
FGF23
Low-transitory FGF23
0.5 nM FGF23 for 1 h
High-prolonged FGF23
10 nM FGF23 for 24 h
RNA-seq and data analysis
E
+Klotho
–Klotho
All
Up
Down
DEG count (padj<0.05)
F
Low-transitory FGF23 +Klotho
Down
Up
EGR1
FOS
JUNB
SPRY4
DUSP6
-log10(padj)
log2FoldChange
G
Low-transitory FGF23 –Klotho
H
EGR1
FOS
ARC
MAFF
PTGS2
GPR3
SPRY4
JUNB
ZFP36
NR4A1
DUSP6
C11orf96
GADD45B
CTGF
F3
padj<0.05
log2FC>1
% change in gene expression
I
GO pathways (padj<0.05; log2FC>1)
transcription factor activity
response to extracellular stimulus
response to peptide hormone
ERK1 and ERK2 cascade
regulation of MAP kinase activity
response to FGF
DEG count

Fig. 2

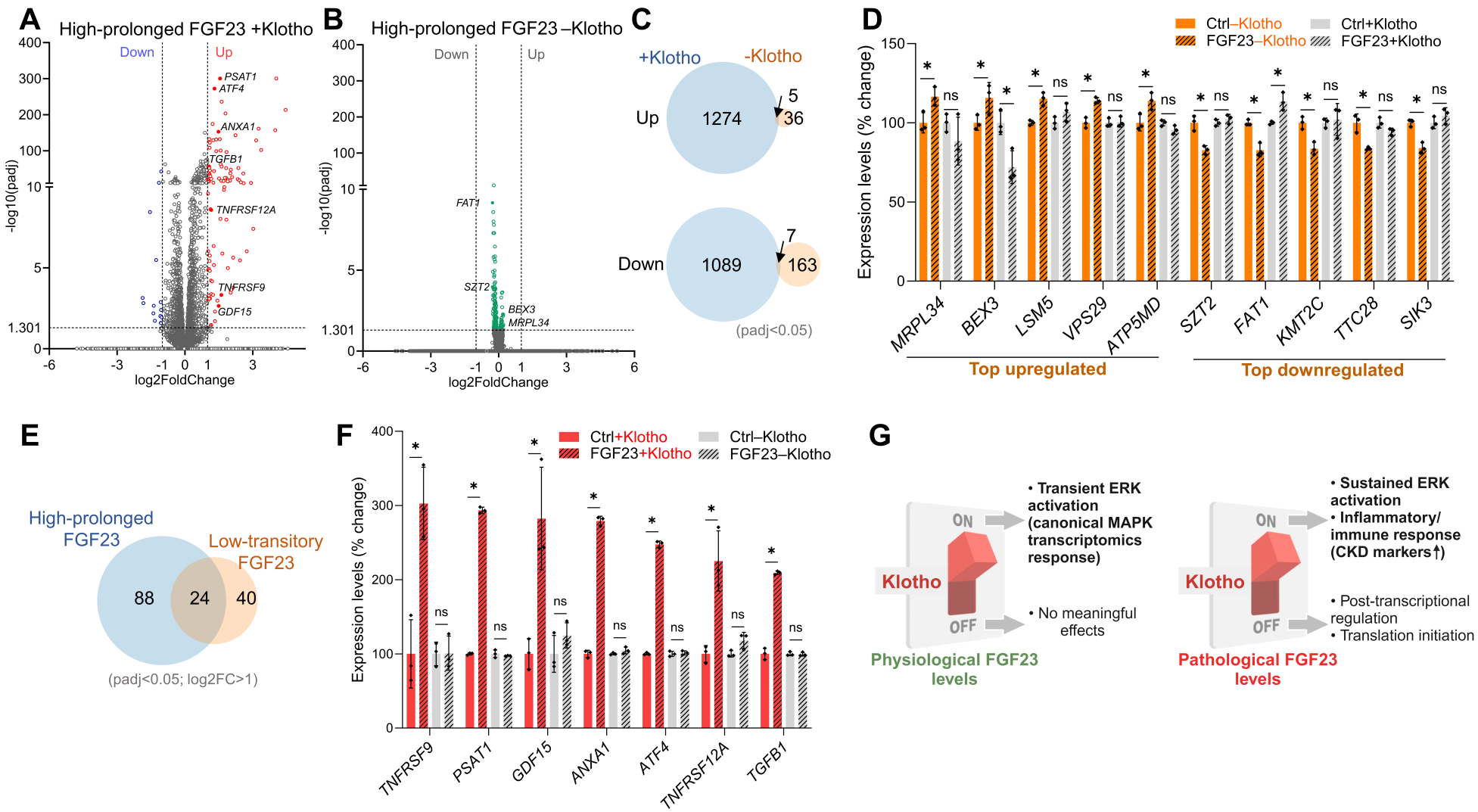
A
High-prolonged FGF23 +Klotho
Down
Up
PSAT1
ATF4
ANXA1
TGFB1
TNFRSF12A
TNFRSF9
GDF15
-log10(padj)
log2FoldChange
B
High-prolonged FGF23 –Klotho
FAT1
SZT2
BEX3
MRPL34
C
+Klotho
-Klotho
Up
1274
5
36
Down
1089
7
163
(padj<0.05)
D
Ctrl–Klotho
FGF23–Klotho
Ctrl+Klotho
FGF23+Klotho
Expression levels (% change)
MRPL34
BEX3
LSM5
VPS29
ATP5MD
SZT2
FAT1
KMT2C
TTC28
SIK3
Top upregulated
Top downregulated
E
High-prolonged FGF23
Low-transitory FGF23
88
24
40
(padj<0.05; log2FC>1)
F
Ctrl+Klotho
FGF23+Klotho
Ctrl–Klotho
FGF23–Klotho
Expression levels (% change)
TNFRSF9
PSAT1
GDF15
ANXA1
ATF4
TNFRSF12A
TGFB1
G
ON
Klotho
OFF
• Transient ERK activation (canonical MAPK transcriptomics response)
• No meaningful effects
Physiological FGF23 levels
• Sustained ERK activation
• Inflammatory/ immune response (CKD markers↑)
• Post-transcriptional regulation
• Translation initiation
Pathological FGF23 levels

Identification of novel and distinct FGF23 signaling in a Klotho-dependent and -independent manner

Klaudia Kopper[1,2], Johanne Pastor[4], Orson W. Moe[3,4,5], Johannes Loffing[1,2], Ganesh Pathare[1,2]*

[1]Institute of Anatomy, University of Zurich, Zurich, Switzerland

[2]Swiss National Centre of Competence in Research "Kidney Control of Homeostasis", Switzerland

[3]Charles and Jane Pak Center for Mineral Metabolism and Clinical Research, University of Texas Southwestern Medical Center, Dallas, Texas, USA.

[4]Departments of Internal Medicine, University of Texas Southwestern Medical Center, Dallas, Texas, USA.

[5]Departments of Physiology, University of Texas Southwestern Medical Center, Dallas, Texas, USA.

***Corresponding author**:

Ganesh Pathare

Institute of Anatomy

University of Zurich

Winterthurerstrasse 190, 8057, CH

Email: ganesh.pathare@anatomy.uzh.ch

Keywords: FGF23, Klotho, chronic kidney disease, left ventricular hypertrophy and inflammation

Competing Interests

The authors declare no potential conflicts of interest.

This PDF file includes:

Supplementary materials and methods

References for methods

Legends for datasets S1 to S8

MATERIALS AND METHODS

All the chemicals were purchased from Sigma Aldrich unless otherwise stated.

Culture of HEK293 cells.

HEK293 cell line ($HEK293^{Wt}$) was originally purchased from ATCC. The cells were cultured in a growth medium consisting of Minimum Essential Medium MEM, with L-Glutamine (gibco; Cat #11095-080) supplemented with 10% heat-inactivated FBS and 100 U/ml penicillin, and 100 µg/ml streptomycin (gibco; Cat. #15140122). Cells between passages 6 and 15 were used in this study.

Generation of $HEK293^{Kl}$ cells.

For deriving stable Klotho cell line ($HEK293^{Kl}$), $HEK293^{Wt}$ cells were transfected with 3 µg of plasmid DNA (Addgene; Cat #17712; http://n2t.net/addgene:17712; RRID:Addgene_17712) in 60 mm culture dish using Jetprime (Polyplus; Cat #55-134) transfection reagent following manufacturer's protocol. Cells stably expressing Klotho were selected using 400 µg/ml of G418. Subsequently, $HEK293^{Kl}$ cells were expanded and tested for Klotho protein and mRNA expression by immunoblotting and qPCR respectively. Then $HEK293^{Kl}$ aliquots were frozen at -150°C until further use.

Treatment with FGF23

Both $HEK293^{Wt}$ and $HEK293^{Kl}$ cells undergo exactly similar experimental conditions. A similar number of $HEK293^{Wt}$ and $HEK293^{Kl}$ cells were seeded in a 6-well plate. After 48 hours, the cells were serum-starved for 16 hours and treated with either vehicle or human recombinant FGF23 (Biotechne; Cat #2604-FG) at specified doses and times mentioned in the results section.

Immunoblotting

Both $HEK293^{Wt}$ and $HEK293^{Kl}$ cells were homogenized in ice-cold RIPA lysis buffer (Thermo Fisher, Cat. #89900). Then cell lysates were centrifuged for 10 min at 2000 g and supernatants were used for immunoblotting. Protein concentration was measured by Bradford assay (CooAssay Protein Dosage Reagent; Uptima, Cat. #UPF86421). Equal amounts of protein (30 µg) were loaded in Laemmli buffer (pH 6.8) on 8% polyacrylamide gels. Electrophoretically separated proteins were blotted to nitrocellulose membranes at 100 V for 2 hours. Next, membranes were blocked in Odyssey blocking buffer (LI-COR; Cat. # 927-70001) for 1 hour. The membrane was further incubated with diluted anti-human Klotho monoclonal antibody/Clone: KM2076 (TransGenic; Cat. #KO603), pERK1/2 (Cell Signaling; Cat #4370S) and tERK1/2 (Cell Signaling; Cat. #4695S) overnight at 4°C. On the following day, diluted secondary antibodies goat-anti-rabbit IRDye 800 (LI-COR; Cat. #926-32211), goat-anti-rat IRDye 800 (LI-COR; Cat. #926-32219) and goat-anti-mouse IRDye 680 (LI-COR; Cat. #926-68070) were added to the membranes in Casein Blocking solution in deionized water (1:10) and incubated for 1 hour at room temperature. Then membranes were repeatedly washed with phosphate-buffered saline containing 0.1% Tween 20. The fluorescent signal was visualized using Odyssey IR imaging system (LI-COR Biosciences).

RNA isolation and qRT-PCR

The RNA was extracted from HEK293^{Wt} and HEK293^{Kl} cells using a Nucleospin RNA isolation kit (Macherry Nagel; Cat. #740955). The RNA was transcribed using a High-Capacity cDNA Reverse Transcription Kit (Thermo Fisher; Cat. #4374966) and subjected to qPCR with SybrGreen Master Mix (Roche; Cat. #4707516001) using the following primers:

hKL-Fwd: GCTTTCCTGGATTGACCTTG
hKL-Rev: TGTAACCTCTGTGCCACTCG
hEGR1-Fwd: AGAAGGACAAGAAAGCAGACAAAAGTGT
hEGR1-Rev: GGGGACGGGTAGGAAGAGAG
hGAPDH-Fwd: ACAACTTTGGTATCGTGGAAGGAC
hGAPDH-Rev: CAGGGATGATGTTCTGGAGAG

The relative quantification of gene expression based on double-delta Ct (threshold cycle) analysis was performed after normalization to *GAPDH* expression. All the gene expression values are expressed as arithmetic means ± SD, where n represents a number of independent experiments (biological replicates). An unpaired Student's t-test was used for comparisons between the groups using GraphPad Prism.

Illustrations

Graphical illustrations were created using a licensed version of Biorender software.

RNA-sequencing and data analysis

Both HEK293^{Wt} and HEK293^{Kl} cells were treated with vehicle (control) and FGF23 for a specified dose and duration. Please refer to fig. 1D for the experimental plan. RNA was isolated using a Nucleospin kit as explained earlier. RNA-seq was performed commercially by Novogene (UK) Company Limited as previously described[1]. In brief, amplified cDNA samples were subjected to different quality control standards. RNA sample was used for library preparation using NEB Next® Ultra RNA Library Prep Kit for Illumina®. Indices were included to multiplex multiple samples. Briefly, mRNA was purified from total RNA using poly-T oligo-attached magnetic beads. After fragmentation, the first strand cDNA was synthesized using random hexamer primers followed by the second strand cDNA synthesis. The library was ready after end repair, A-tailing, adapter ligation, and size selection. After amplification and purification, the insert size of the library was validated on an Agilent 2100 and quantified using quantitative qPCR. Libraries were then sequenced on Illumina NovaSeq 6000 S4 flow cell with PE150 according to results from library quality control and expected data volume. We included 24 datasets in the RNA-Seq data analysis, three biological replicates in each group. List of eight experimental groups as follows: (1) Kl_FGF23_1h; (2) Kl_Ctrl_1h; (3) WT_FGF23_1h; (4) WT_Ctrl_1h; (5) Kl_FGF23_24h; (6) Kl_Ctrl_24h; (7) WT_FGF23_24h; (8) WT_Ctrl_24h.

The fold changes were calculated by dividing the arithmetic mean of the normalized read counts by the number of replicates. The statistical significance of differential gene expression in RNA-Seq data was determined with padj value<0.05. Please refer to the legends for the datasets to find more information about each dataset. Venn diagrams for the sets of genes up- or down-regulated were made by intersecting the lists of gene names between control and FGF23 treatment in $HEK293^{Kl}$ and $HEK293^{Wt}$ cells (R package VennDiagram version 1.71). The input expression matrix was normalized by row (gene) by computing a z-score. Both experimental groups (columns) and gene expression profiles (rows) were clustered using the euclidean distance and the hierarchical clustering algorithm. Gene set groups were obtained by cutting the dendrogram in eight slices with the cutree default implementation of the Heatmap function. Functional over-representation analysis of gene ontology biological processes was performed with the R package clusterProfiler (version 3.16.1) using as input the genes up/downregulated upon FGF23 treatment (padj<0.05) and considering a significance q-value cutoff of 0.05.

DATA AVAILABILITY

All the relevant data associated with the current study can be found in the main text or supplementary datasets. The raw RNA-seq data used in this publication have been deposited in NCBI's Gene Expression Omnibus and are accessible through GEO Series accession number GSE248734 (https://www.ncbi.nlm.nih.gov/geo/query/acc.cgi?acc=GSE248734). All data are available from the authors upon reasonable request.

REFERENECS

1. Radvanyi, Z., Yoo, E. J., Kandasamy, P., Salas-Bastos, A., Monnerat, S., Refardt, J., Christ-Crain, M., Hayashi, H., Kondo, Y., Jantsch, J., Rubio-Aliaga, I., Sommer, L., Wagner, C. A., Hediger, M. A., Kwon, H. M., Loffing, J. & Pathare, G. Extracellular sodium regulates fibroblast growth factor 23 (FGF23) formation. *J. Biol. Chem.* 105480 (2023) doi:10.1016/J.JBC.2023.105480.

LEGENDS FOR DATASETS S1 TO S8

Dataset S1: List of all the genes identified upon low-transitory FGF23 in HEK293^{KI} cells.

Dataset S2: List of all the genes identified upon low-transitory FGF23 in HEK293^{Wt} cells.

Dataset S3: List of all the GO pathways implicated upon low-transitory FGF23 in HEK293^{KI} cells.

Dataset S4: List of all the genes identified upon high-prolonged FGF23 in HEK293^{KI} cells.

Dataset S5: List of all the genes identified upon high-prolonged FGF23 in HEK293^{Wt} cells.

Dataset S6: List of the common genes when compared between high-prolonged FGF23 in HEK293^{KI} *versus* high-prolonged FGF23 in HEK293^{Wt} cells.

Dataset S7: List of all the GO pathways implicated upon high-prolonged FGF23 in HEK293^{Wt} cells.

Dataset S8: List of the unique genes when compared between high-prolonged *versus* low-transitory FGF23 in HEK293^{KI} cells.